arXiv:2411.11108v1 [eess.SY] 17 Nov 2024

Iterative Learning Control for Ramp Metering on Service Station On-ramps

Hongxi Xiang[1], Carlo Cenedese[2,3], Efe C. Balta[2,4], and John Lygeros[2]

***Abstract*— Congestion on highways has become a significant social problem due to the increasing number of vehicles, leading to considerable waste of time and pollution. Regulating the outflow from the Service Station can help alleviate this congestion. Notably, traffic flows follow recurring patterns over days and weeks, allowing for the application of Iterative Learning Control (ILC). Building on these insights, we propose an ILC approach based on the Cell Transmission Model with service stations (CTM-s). It is shown that ILC can effectively compensate for potential inaccuracies in model parameter estimates by leveraging historical data.**

I. INTRODUCTION

Traffic congestion in modern cities presents a major challenge for reducing emissions and combating climate change. Despite the emergence of alternative transportation options, roads remain the primary mode of transport for both people and goods in the US and EU [1], with demand predicted to increase by 42% by 2050 [2]. Beyond the environmental impact and the related health risks, congestion leads to significant economic losses due to inefficiencies, such as increased fuel consumption and delayed delivery of goods [3]. Since naive solutions such as increasing capacity are not scalable, research has focused on optimizing the existing infrastructure. This approach requires a smaller investment and is adaptable to changing traffic conditions.

The optimal operation of highway networks has long been a focus of research due to its significant impact on overall traffic. Numerous strategies have been proposed to reduce congestion [4, 5], with on-ramp metering management emerging as one of the most effective ones [6, 7].

While highway on-ramp management has been well-studied, the role of Service Stations (STs) and their influence on traffic has gained attention only recently. In [8, 9], the authors proposed the "Cell Transmission Model with service stations" (CTM-s), showing that (if located strategically), a ST can reduce the peak traffic congestion on the highway stretch, acting as a damper preventing the congestion wave propagation. In [10] a second-order model based on METANET was proposed together with a simple control strategy based on ALINEA to regulate the flow of vehicles merging back into the mainstream from the ST. These previous works did not consider the repetitive nature of the traffic demand, which makes the problem inherently well-suited for learning-based control strategies such as Iterative Learning Control (ILC).

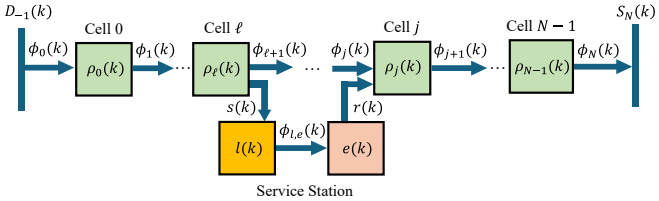

Fig. 1: Illustration of CTM-s model with one ST.

ILC is a control strategy for iterative tasks, where the measurements of previous iterations are used for improving the control performance of subsequent iterations. ILC was originally formulated as an unconstrained tracking problem [11, 12]. To tackle constraints systematically, the Optimization-based ILC (OB-ILC) was then developed [13, 14], with theoretical results including convergence analyses shown in [15], [16]. These results do not consider noise or model mismatch, both crucial features of real-world applications. Adaptive ILC methods are developed to deal with parametric uncertainties in discrete-time repetitive systems [17, 18]. [19] develops a scheme for discrete-time non-repetitive systems subject to iteration-varying unknown parameters and variable initial conditions. In [20], adaptation is achieved by combining ILC with Reinforcement Learning. However, none of these methods provides robust constraint satisfaction guarantees. Recent work in [21] develops an OB-ILC scheme that uses a robust operator-theoretic framework to provide constraint satisfaction in the presence of noise and modeling errors for linear systems, also studied for iteration-varying systems [22].

The main contributions of this paper are: (**i**) The first Model Predictive Control (MPC) based ramp metering scheme using CTM-s to control the flow exiting a ST to reduce the mainstream congestion; (**ii**) a novel ILC scheme for highway traffic control, where we systematically integrate previous traffic data into the controller design to improve performance. Our approach relaxes the knowledge and modeling requirements by providing means to compensate for parameter estimation errors. The efficacy of our ILC scheme is validated via numerical studies demonstrating convergence to the correct parameter values and performance improvement.

This work was supported as a part of NCCR Automation, a National Centre of Competence in Research, funded by the Swiss National Science Foundation (grant number 51NF40_225155)

[1] Department of Mechanical and Process Engineering at ETH Zürich, Zürich, Switzerland. Email: hxiang@student.ethz.ch.

[2] Department of Information Technology and Electrical Engineering at ETH Zürich, Zürich, Switzerland. Email: lygeros@control.ee.ethz.ch.

[3] Delft Center for Systems and Control, Delft University of Technology, Delft, The Netherlands. Email: ccenedese@tudelft.nl

[4] inspire AG, Zürich, Switzerland. Email: efe.balta@inspire.ch

II. CTM-S DYNAMICS

In this section, we adapt the CTM-s model introduced in [8, 9] to our context. In the model, time is discretized into intervals $[kT, (k+1)T)$ of length T indexed by $k \in \mathbb{N}$, and the highway stretch is divided into N consecutive cells indexed by $i \in \mathcal{N} = \{0, ..., N-1\}$, see Fig. 1. The vehicles exiting cell i during the interval k can either enter the subsequent cell $i+1$ or exit using an off-ramp if available. Similarly, new vehicles can enter cell i from either cell $i-1$ or an on-ramp. The CTM-s exploits the presence of on and off ramps to model the presence of a ST. For simplicity, we assume there is only a single ST identified by the pair (ℓ, j), where $\ell, j \in \mathcal{N}$, with ℓ and j denoting the exit and merge cells to the ST, respectively.

Differently from [8], we model separately the vehicles actively using the service station $l(k)$ and those waiting in a queue while merging back from the ST, $e(k)$. Moreover, we consider a highway stretch with no other ramps. It is important to emphasize that the following methodology can also be applied to more general cases, at the expense of more convoluted notation. Please refer to [8] for an in-depth discussion of the model and possible generalizations that relax these assumptions.

Next, we report the dynamics of the model using the variables in Table I. We divide the dynamics into linear and non-linear, which will be useful for controller design.

1) Linear dynamics. The following dynamics guarantee the conservation of the number of vehicles and represent the cornerstone of the model. The density in cell i evolves as

$$\rho_i(k+1) = \rho_i(k) + \frac{T}{L_i}\left(\Phi_i^+(k) - \Phi_i^-(k)\right), \tag{1}$$

where the total inflow and outflow are

$$\Phi_i^+(k) = \phi_i(k) + r_i(k), \tag{2a}$$
$$\Phi_i^-(k) = \phi_{i+1}(k) + s_i(k). \tag{2b}$$

Notice that $s_i(k) = s(k) = \beta\Phi_i^-(k-1)$ if $i = \ell$ and 0 otherwise, similarly $r_i(k) = r(k)$ only if $i = j$ and 0 otherwise. Vehicles spend on average δ time intervals ($\delta\, T$) receiving service within the station before joining the queue to exit, thus

$$l(k+1) = l(k) + T(s(k) - \phi_{l,e}(k)), \tag{3a}$$
$$e(k+1) = e(k) + T(\phi_{l,e}(k) - r(k)), \tag{3b}$$
$$\phi_{l,e}(k) = s(k-\delta). \tag{3c}$$

2) Non-linear dynamics. The nonlinearities in the model are due to the flows among cells defined by the minimum between the upstream demand and downstream supply. The demand and supply for the cells and ST are defined as

$$D_i(k) = \min((1-\beta_i)v_i\rho_i(k), q_i^{\max}), \tag{4a}$$
$$S_i(k) = \min(w_i(\rho_i^{\max} - \rho_i(k)), q_i^{\max}), \tag{4b}$$
$$D^s(k) = \min\left(\phi_{l,e}(k) + \frac{e(k)}{T}, r^{\max}\right), \tag{4c}$$

where in (4a), $\beta_i = \beta$ if $i = \ell$ and $\beta_i = 0$ otherwise.

Name	Symbol	Unit	Description
Cell parameters	L_i	[km]	Cell length
	v_i	[km/h]	Free-flow speed
	w_i	[km/h]	Congestion wave speed
	$q_i^{\max}$	[veh/h]	Flow capacity
	$\rho_i^{\max}$	[veh/km]	Jam density
ST parameters	$l^{\max}$	[veh]	Service station capacity
	$e^{\max}$	[veh]	Queue length capacity
	$r^{\max}$	[veh/h]	On-ramp capacity
	$\delta\, T$	[h]	Average time spent at ST
	β	[-]	Split ratio at cell ℓ
	p^{ms}	[-]	Priority of mainstream
Cell variables	$\rho_i(k)$	[veh/km]	Density of cell i
	$\Phi_i^+(k)$	[veh/h]	Total inflow into cell i
	$\Phi_i^-(k)$	[veh/h]	Total outflow from cell i
	$\phi_i(k)$	[veh/h]	Flow from cell $i-1$ to i
	$D_i(k)$	[veh/h]	Demand of cell i
	$S_i(k)$	[veh/h]	Supply of cell i
ST variables	$l(k)$	[veh]	Number of vehicles in ST
	$e(k)$	[veh]	Queue length
	$s(k)$	[veh/h]	Inflow to ST
	$\phi_{l,e}(k)$	[veh/h]	Flow from $l(k)$ to $e(k)$
	$D^s(k)$	[veh/h]	Demand of ST
	$r(k)$	[veh/h]	On-ramp flow from ST
Boundary conditions	$D_{-1}(k)$	[veh/h]	Initial upstream demand
	$S_N(k)$	[veh/h]	Downstream supply

TABLE I: CTM-s parameters and variables

For all $i \neq j$, the flow between cell $i-1$ and i reads as

$$\phi_i(k) = \min(D_{i-1}(k), S_i(k)). \tag{5}$$

On the contrary, if $i = j$, the supply of cell i is shared by ST and cell $i-1$, so

$$\phi_i(k) = \min(D_{i-1}(k), S^{\text{ms}}(k)), \tag{6}$$

where $S^{\text{ms}}(k) := \max(S_i(k) - D^s(k)), p^{\text{ms}}S_i(k))$, this formulation replaces the use of the *middle* operator, used in [3, Eq. 3.34]. Similarly, we can compute $r(k)$ as follows

$$r(k) = \min(D^s(k), S^{\text{ST}}(k)), \tag{7}$$

where $S^{\text{ST}}(k) := \max(S_j(k) - \phi_j(k), (1-p^{\text{ms}})S_j(k))$ denotes the remaining supply of cell j available to the vehicles that aim to merge back.

As boundary conditions, we impose that $D_{-1}(k)$ is the exogenous upstream demand and that $S_N(k) = +\infty$, hence no downstream bottleneck influences the flow on the considered highway stretch.

III. ST RAMP METERING

In this section, we formulate two controllers for ramp metering on the on-ramp allowing vehicles to exit the ST. First, we formulate an MPC that uses the CTM-s to optimally restrict the ST's outflow to reduce the overall traffic congestion. Then, we augment this with an ILC scheme, where we leverage the repetitiveness of the traffic demand.

A. MPC formulation

Ramp metering schemes based on MPC have proven effective in real-life experiments [23]. In the case of ST, the MPC controller directly influences $D^s(k)$ via the input $r_c(k)$ that controls the maximum number of vehicles that can exit the ST during the interval k. Therefore, the ST demand in (4c) when the control is active becomes

$$D^s(k) = \min\left(\phi_{l,e}(k) + \tfrac{e(k)}{T}, r^{\max}, r_c(k)\right). \tag{8}$$

The standard MPC formulation requires defining a cost function J to be minimized during the current time interval k_0, over a prediction horizon of length K, subject to constraints associated with the model dynamics and inputs. We consider a linear MPC for efficient computation and approximate the nonlinear CTM-s dynamics to attain only linear constraints.

1) Constraints. The nonlinear part of the CTM-s dynamics arises from (4)–(8). Inspired by [24], we linearize these equations by relaxation. For all $i \neq j$, we relax (5) as

$$\phi_i(k) \leqslant \min(D_{i-1}(k), S_i(k)), \tag{9}$$

where the two are equivalent if (9) is active. Substituting (4a) and (4b) into (9) leads to

$$\phi_i(k) \leqslant (1-\beta_{i-1})v_{i-1}\rho_{i-1}(k), \tag{10a}$$
$$\phi_i(k) \leqslant q_{i-1}^{\max}, \tag{10b}$$
$$\phi_i(k) \leqslant w_i(\rho_i^{\max} - \rho_i(k)), \tag{10c}$$
$$\phi_i(k) \leqslant q_i^{\max}. \tag{10d}$$

Similarly, for $i = j$ we relax (6), (7) and (8) as

$$\phi_i(k) \leqslant (1-\beta_{i-1})v_i\rho_{i-1}(k), \tag{11a}$$
$$\phi_i(k) \leqslant q_{i-1}^{\max}, \tag{11b}$$
$$r(k) \leqslant \phi_{l,e}(k) + e(k)/T, \tag{11c}$$
$$r(k) \leqslant r^{\max}, \tag{11d}$$
$$\phi_i(k) + r(k) \leqslant w_i(\rho_i^{\max} - \rho_i(k)), \tag{11e}$$
$$\phi_i(k) + r(k) \leqslant q_i^{\max}, \tag{11f}$$

where (11a) and (11b) constrain $\phi_i(k)$ by the demand of cell $i-1$, while (11c) and (11d) constrain $r(k)$ by the demand of ST. Finally, (11e) and (11f) indicate that the sum of the two is constrained by the supply of the next cell i.

Notice the approximation above ignores p^{ms}, i.e., we only consider the first terms in both $S^{\text{ms}}(k)$ and $S^{\text{ST}}(k)$. In practice, p^{ms} is usually close to 1 hence the mainstream flow has a higher priority than the flow from the ST. We promote this behavior in our controller by weighting $\phi_i(k)$ more than $r(k)$ in the cost function design, as detailed in the next section.

Among the controller's goals, we also include limiting the maximum queue length at the exit of the ST. This can be imposed via the following constraint

$$e(k) \leqslant e^{\max}, \tag{12}$$

where $e^{\max}$ is the fixed maximum queue length.

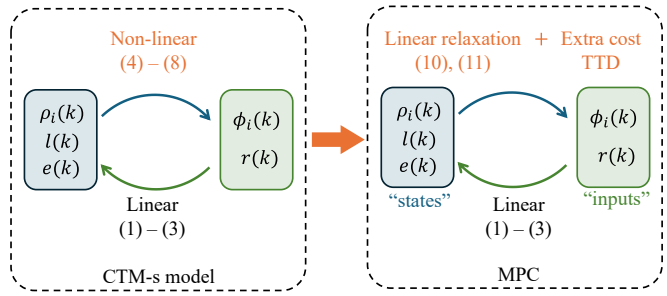

Fig. 2: Relations between CTM-s model and MPC formulation. The non-linear dynamics (4) - (8) are relaxed as linear constraints (10), (11) with an extra cost term TTD. Moreover, the variables in blue boxes are known at time step k, while those in green boxes are only known after $k+1$. Thus, they are defined as states and inputs, respectively.

2) Cost function. The primary control objective is to minimize the traffic congestion on the highway stretch. As the congestion metric, we use the Total Travel Time (TTT) over the whole prediction horizon, which is a widely used metric in highway control in the literature, e.g., see [3, Ch.8], and it is defined as

$$\text{TTT}(k_0, k_0+K) := \textstyle\sum_{k=k_0}^{k_0+K}\sum_{i=0}^{N-1}\rho_i(k)L_i. \tag{13}$$

To compensate for the relaxed constraints, we design a cost function to push the variables against the constraint (10) - (11). This approach leads to optimal solutions that satisfy a subset of the constraints with equality, which, in turn, satisfy the original non-linear CTM-s dynamics. To this end, we maximize the flows $\phi_i(k)$ and $r(k)$. Therefore, the cost J minimized by the MPC becomes

$$\text{TTT}(k_0, k_0+K) - \lambda \sum_{k=k_0}^{k_0+K-1}\left(w_r r(k) + \sum_{i=0}^{N}\phi_i(k)L_{i-1}\right), \tag{14}$$

where $\lambda > 0$ and small w_r $(0 < w_r < L_{j-1})$ gives priority to the mainstream flow $\phi_j(k)$ when merging. The last term in (14) is called Total Travel Distance (TTD), see [3, Ch.8]. Since there is no cell -1, we set L_{-1} to a predefined weight. Note that during the control horizon $[k_0T, (k_0+K)T]$, the flows $\phi_i(k_0+K)$ and $r(k_0+K)$ have not taken place yet, since by definition, they are flows during $[(k_0+K)T, (k_0+K+1)T)$. Therefore, the flows are only summed up to K_0+K-1 instead of k_0+K. For the same reason, in the following section, we define $\phi_i(k)$ as part of the inputs in the MPC formulation, even though we only regulate $r(k)$, since there are no initial values for them to propagate the dynamics, see Fig. 2.

3) Overall formulation. To formulate the linear MPC, we first organize the CTM-s variables as states $x(k) := [\rho_0(k), \dots \rho_{N-1}(k), l(k), e(k)]^\top \in \mathbb{R}^{N+2}$, and inputs $u(k) := [\phi_0(k), \dots, \phi_N(k), r(k)]^\top \in \mathbb{R}^{N+2}$. Then the collection of the variables over the prediction horizon is denoted by $x_{k_0} := \text{col}\left(\{x(k_0+k)\}_{k=0}^{K}\right) \in \mathbb{R}^{(N+2)\times(K+1)}$

and $u_{k_0} := \mathrm{col}\left(\{u(k_0+k)\}_{k=0}^{K-1}\right) \in \mathbb{R}^{(N+2)\times K}$, $\phi_{l,e,k_0} := \mathrm{col}\left(\{\phi_{l,e}(k_0+k)\}_{k=0}^{K-1}\right) \in \mathbb{R}^{K}$.

The MPC at time at time k_0 reads as

$$\min_{u_{k_0}} J(u_{k_0}) = \tfrac{a}{2}\|x_{k_0} - x_r\|_Q^2 + c_x^\top x_{k_0} - c_u^\top u_{k_0}, \quad (15a)$$

$$\text{s.t.} \quad x_{k_0} = x_{\text{init},k_0} + G u_{k_0} + G_h\ \phi_{l,e,k_0}, \quad (15b)$$

$$A_x x_{k_0} + A_u u_{k_0} \leqslant b_{k_0}, \quad (15c)$$

$$x_{k_0} \geqslant 0, u_{k_0} \geqslant 0. \quad (15d)$$

In the objective function (15a), the two linear cost terms correspond to (14). Moreover, we augment the cost with an additional quadratic term to provide necessary gradient information for the ILC scheme devised in the next section. However, this quadratic term should be designed carefully since it potentially diverges the optimal solution from satisfying the subset of relaxed constraints (10) and (11) with equality. Since we are to minimize x, we set $x_r := 0$ in our implementation. We further define a diagonal $Q > 0$, where its diagonal elements associated with $\rho_i(k)$, $l(k)$, and $e(k)$ are set to $w_\rho L_i/\rho_i^{\max}$, $w_l/l^{\max}$, and $w_e/e^{\max}$, with weights w_ρ, w_l, $w_e > 0$ normalized by $\rho_i^{\max}$, $l^{\max}$, and $e^{\max}$, respectively. This ensures that the quadratic terms behave approximately linearly to conserve the tightness of the optimal solution at the subset of relaxed constraints (10) and (11) as much as possible. The predefined $a > 0$ is then used to achieve a reasonable trade-off between the gradient information and inaccuracy induced by relaxation.

In (15b), $x_{\text{init},k_0} := \mathbb{1} \otimes x(k_0)$ with $\mathbb{1}$ as a vector of ones of the correct dimension. The constraints (1) – (3), (10) – (12) are included in compact form in (15b), (15c) and (15d), where G, G_h, A_x, A_u are matrices of the correct dimensions.

In practice, the time sampling interval T is a design choice, and highway parameters L_i, v_i, w_i, $q_i^{\max}$, $r^{\max}$ are constant and can usually be measured precisely. However, the split ratio β, average waiting time δ, and future initial demand $D_{-1}(k)$ depend on the drivers and are difficult to estimate. Therefore, (15) is solved by using the best estimates β_{es}, δ_{es}, and $D_{-1,\text{es}}(k)$ of the corresponding parameters, i.e., (15b) and (15c) are substituted by

$$x_{k_0} = x_{\text{init},k_0} + M u_{k_0} + G_h\ \phi_{l,e,k_0,\text{es}}, \quad (16a)$$

$$A_{x,\text{es}} x_{k_0} + A_u u_{k_0} \leqslant b_{\text{es}}, \quad (16b)$$

where M, $A_{x,\text{es}}$, b_{es}, and $\phi_{l,e,k_0,\text{es}}$ are estimates of G, A_x, b, and ϕ_{l,e,k_0}, respectively, based on estimates β_{es}, δ_{es}, and $D_{-1,\text{es}}(k)$.

After solving the MPC problem, we set the obtained optimal input $r^*(k)$ as the control input $r_c(k)$ in (8). Typically, in an MPC setting, the control input is updated at every time step. However, empirical experiments suggest that increasing the update interval has minimal impact on control performance. In our implementation, we update the control input every p steps to reduce the computation load.

B. ILC formulation

1) Motivation for ILC. As we will see in simulations, poor estimates β_{es}, δ_{es}, and $D_{-1,\text{es}}(k)$ can significantly undermine performance. To improve performance over time, we exploit the approximately repetitive nature of the problem. Specifically, the traffic pattern on the highway repeats from day to day and from week to week, enabling us to "learn" and "improve" the estimates of the unknown parameters based on previous data.

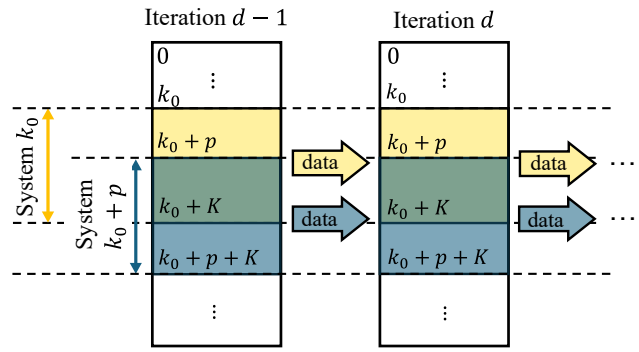

Fig. 3: General framework of applying ILC to highway traffic. Yellow and blue boxes denote *system* k_0 and *system* k_0+p (with horizon length K), respectively. We compute the control inputs for system k_0 on iteration d by (17) using data of the same system on iteration $d-1$. Then we apply the control inputs until updated at time step k_0+p for the next system.

2) The control framework. Figure 3 illustrates how the ILC framework is implemented for highway traffic control. For simplicity, we assume that the traffic pattern repeats daily, though our approach can be easily adapted to any period.

We implement ILC in a receding-horizon fashion. For computing control actions at time step k_0 of iteration d, i.e., the d-th day, we use the data of time steps $k \in [k_0, k_0+K]$ collected during the previous iteration $d-1$. We update control inputs every p time step. Therefore, at time step k_0+p, the control inputs are recomputed using the data of $k \in [k_0+p, k_0+p+K]$ of the previous iteration. This process repeats until the entire desired control period is covered.

We call the traffic between k_0 and k_0+K (denoted by the yellow boxes in Fig. 3) *system* k_0, which corresponds to the nominal problem (15) at k_0. Similarly, we call the traffic between k_0+p and k_0+p+K (denoted by blue boxes in Fig. 3) *system* k_0+p, and so on.

Note that we iterate horizontally rather than vertically. This is because the repetitive pattern of highway traffic occurs simultaneously on each iteration (e.g., day), while the traffic during a single iteration (e.g., during one day) can vary largely at different time steps. For example, the traffic demand during the morning peak strongly differs from one in the evening, see Fig. 4, on the contrary, the morning peak traffic demand on one day is usually similar to one of the previous day.

We propose an ILC formulation based on [21] and focus on a particular system k_0 and omit the subscript "k_0" if there is no ambiguity. The subscript d denotes the iteration index.

3) Formulation. Based on (15), we propose the following ILC formulation.

$$\min_{v} \ \tfrac{1}{2}\|v - u_{d-1}\|_W^2 + \alpha\, v^\top F(x_{d-1}, u_{d-1}), \quad (17a)$$

$$s.t. \quad x_d = Mv + x_{\text{init},d} + x_{d-1} - Mu_{d-1} - x_{\text{init},d-1}, \quad (17b)$$
$$A_{x,es}x_d + A_u v \leqslant b_{d-1}, \quad (17c)$$
$$x_d \geqslant 0 \quad v \geqslant 0, \quad (17d)$$

where u_{d-1}, x_{d-1} are measurements from the previous iteration. Additionally b_{d-1} uses previous data $D_{-1,d-1}(k)$ and $\phi_{l,e,d-1}(k)$. For the objective (17a), $W := M^\top QM \succ 0$ is a preconditioner matrix. Note that in our formulation, M has full column rank, therefore it is guaranteed that $W \succ 0$ as long as $Q \succ 0$. $\alpha > 0$ is a predefined weight and F is an approximation of the gradient of the nominal objective function (15a), defined next.

For iteration d, by replacing (15a) into (15b), we attain

$$J_d(u) = \frac{1}{2}u^\top Hu + f_d^\top u + c, \quad (18)$$

where $H := a\, G^\top QG$, $f_d := a\, G^\top Q(w_d - x_r) + G^\top c_x - c_u$, $w_d := G_h\phi_{l,e_d} + x_{\text{init,d}}$, and $c := G^\top c_x - c_u$. Then we have

$$\begin{aligned}\nabla J_d(u) &= Hu + f_d \\ &= a\,[G^\top Q(Gu + w_d - x_r)] + G^\top c_x - c_u. \quad (19)\end{aligned}$$

Since we do not know G, and w_d exactly, we define

$$F(x_{d-1}, u_{d-1}) := a\,[M^\top Q(x_{d-1} - x_r)] + M^\top c_x - c_u \quad (20)$$

as an approximation of the gradient of the objective function of iteration d evaluated at input u of iteration $d-1$, as

$$\nabla J_d(u_{d-1}) = a\,[G^\top Q(Gu_{d-1} + w_d - x_r)] + G^\top c_x - c_u,$$

where we replaced the unknown G with its estimate M and $Gu_{d-1} + w_d$ by x_{d-1}. This is equivalent to replacing w_d by w_{d-1}, since $x_{d-1} = Gu_{d-1} + w_{d-1}$, according to (15b).

Next, we provide the intuition behind constraint (17b). Let $x_{d,GT}$ denote the ground truth values computed by using exact parameters, i.e., $x_{d,GT} = x_{\text{init, d}} + Gv + G_h\phi_{l,e,d}$, then the computation error when using (17b) reads as

$$\begin{aligned}\text{err}_d :=& x_{d,GT} - x_d \\ =& x_{\text{init, d}} + Gv + G_h\phi_{l,e,d} \\ &- (Mv + x_{\text{init},d} + x_{d-1} - Mu_{d-1} - x_{\text{init},d-1}) \\ =& (G - M)(v - u_{d-1}) + G_h(\phi_{l,e,d} - \phi_{l,e,d-1}), \quad (21)\end{aligned}$$

where the last equality comes from $x_{d-1} = Gu_{d-1} + x_{\text{init},d-1} + G_h\phi_{l,e,d-1}$. Therefore, since from (17a) we try to minimize the distance between v and u_{d-1}, then the estimated error $G - M$ will be compensated.

After computing (17), we apply the optimal solution $r^*(k)$ for p time intervals as $r_c(k)$, and then compute a new control input sequence by solving a new instance of (17) associated with the next system.

IV. Simulations

A. Simulations setup

We consider a highway stretch identified by the parameters in Table III. There is a notable reduction of w_i and $q_i^{\max}$ from cell 8 to 9, which creates a bottleneck. The ST is placed upstream of the bottleneck, between cells $\ell = 4$ and $j = 6$, to affect traffic congestion induced by the bottleneck. For further details on the optimal ST placement refer to [9].

	$\mathbf{r}_\beta$	$\mathbf{r}_\delta$	$\mathbf{r_D}$
Underest.	0.8	0.8	0.8
Overesti.	1.2	1.2	1.2

TABLE II: The scaling factors used in the six simulations scenarios to impose under or overestimation errors.

The upstream demand $D_{-1}(k)$ is as in Fig. 4 that is a scaled version of the flow along the A2 highway in the Netherlands during a standard weekday, extracted from the *Nationaal Dataportaal Wegverkeer* [25]. In the simulations, $D_{-1}(k)$ is set to be the same for all days, one iteration corresponds to one day. We focus only on the morning peak from $07:00$ to $10:00$, the initial and final time of the considered peak are denoted by t_s and t_e, respectively. We model the error in the initial estimates of β, δ, and $D_{-1}(k)$, by the scaling factors r_β, r_δ, $r_D \geqslant 0$. The estimated parameters are

$$\beta_\text{es} = r_\beta\beta, \quad \delta_\text{es} = r_\delta\delta, \quad D_{-1,\text{es}}(k) = r_D D_{-1}(k), \quad (22)$$

where a scaling greater or smaller than 1 denotes an over- or underestimation of the corresponding parameter. Our goal is to show that over the iterations, the ILC compensates for this estimation error and achieves performance similar to the ones of the Ground-Truth MPC (GT-MPC), that is the MPC in (15) with the correct parameters in Table III and $D_{-1}(k)$.

B. Controllers and performance metrics

We consider six different scenarios where the parameters in (22) take values as in Table II. Notice that, during the first day ($d = 0$), the ILC scheme cannot be applied, as there is no prior day's data available. Therefore, an MPC is used with parameters β_es, δ_es, and $D_{-1,\text{es}}$.

Since our primary goal is to reduce congestion, we use $\text{TTT}(t_\text{s}, t_\text{e})$ as main evaluation metric. The controller trad offs between alleviating congestion and maintaining a low waiting time at the ST exit. Thus, we consider two additional metrics the Total Waiting Time (TWT) and the Total Time Spent (TTS), defined as

$$\text{TWT}(t_\text{s}, t_\text{e}) := \sum_{k=t_\text{s}}^{t_\text{e}} e(k), \quad (23a)$$
$$\text{TTS}(t_\text{s}, t_\text{e}) := \text{TTT}(t_\text{s}, t_\text{e}) + \text{TWT}(t_\text{s}, t_\text{e}). \quad (23b)$$

TWT measures the waiting time for vehicles at the ST exit, while TTS represents the overall time for traveling and waiting. Moreover, to better assess the convergence performance of ILC to GT-MPC, we define the following relative indices

$$\Delta_\text{TTT} := \text{TTT}^\text{ILC}(t_\text{s}, t_\text{e}) - \text{TTT}^\text{GT-MPC}(t_\text{s}, t_\text{e}), \quad (24a)$$
$$\Delta_\text{TWT} := \text{TWT}^\text{ILC}(t_\text{s}, t_\text{e}) - \text{TWT}^\text{GT-MPC}(t_\text{s}, t_\text{e}), \quad (24b)$$
$$\Delta_\text{TTS} := \text{TTS}^\text{ILC}(t_\text{s}, t_\text{e}) - \text{TTS}^\text{GT-MPC}(t_\text{s}, t_\text{e}), \quad (24c)$$

where the superscript indicates the controller used. Finally, we define the maximum rate of violating the queue length

	i	L_i	v_i	w_i	$q_i^{\max}$	$\rho_{\max}^i$
Cells	0	0.65	103	31	1870	79
	1	0.56	103	25	1735	86
	2	0.61	103	33	1876	75
	3	0.23	103	26	1757	84
	4	0.34	103	33	1780	71
	5	0.54	103	35	1847	71
	6	0.29	103	38	1985	72
	7	0.31	103	40	2092	73
	8	0.59	103	40	2002	69
	9	0.6	96	29	1714	77
	10	0.41	96	29	1705	76
	11	0.2	103	33	1845	74
	12	0.7	103	35	1924	74
	13	0.53	104	30	1774	77
	14	0.51	103	27	1789	83
ST	$l^{\max}$	$e^{\max}$	$r^{\max}$	δ	β	p^{ms}
	400	20	1500	480	0.1	0.9
Other	T [s]	K	p	λ	a	α
	10	90	30	0.5	1	1
	w_ρ	w_e	w_l	w_r	L_{-1}	
	1	0.1	0.05	0.1	0.5	

TABLE III: Parameters of the CTM-s and the controller used in the simulations.

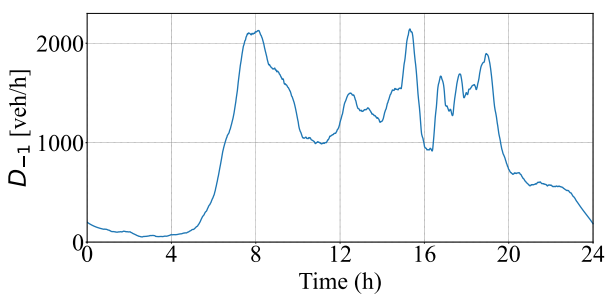

Fig. 4: Initial upstream demand $D_{-1}(k)$.

constraint (12) over $[t_s, t_e]$ as

$$\Delta_{e^{\max}}(t_s, t_e) := \max_{k \in [t_s, t_e]} \left(\frac{\max\left(e(k) - e^{\max}, 0\right)}{e^{\max}} \right). \quad (25)$$

If there is never a violation, then $\Delta_{e^{\max}} = 0$.

C. Results

Table IV shows the results for the highway without control and under the control of GT-MPC. Notice that TTS are almost equal in both cases, indicating the trade-off between TTT and TTS, as expected. Thanks to its precise knowledge of the parameters, GT-MPC is effective, as it reduces congestion (attain lower TTT) while maintaining $\Delta_{e^{\max}} = 0$.

Figure 5 shows the relative performance of ILC in the six scenarios summarized in Table II. Note that the first three subfigures are presented on a logarithmic scale. At iteration 0, since MPC with estimated parameters is applied, the positive

	TTT	**TWT**	**TTS**	$\mathbf{\Delta_{e^{\max}}}$
Uncontrolled	358.49	0.55	359.04	0
GT-MPC	344.64	14.63	359.27	0

TABLE IV: Performance of uncontrolled stretch and the one under GT-MPC.

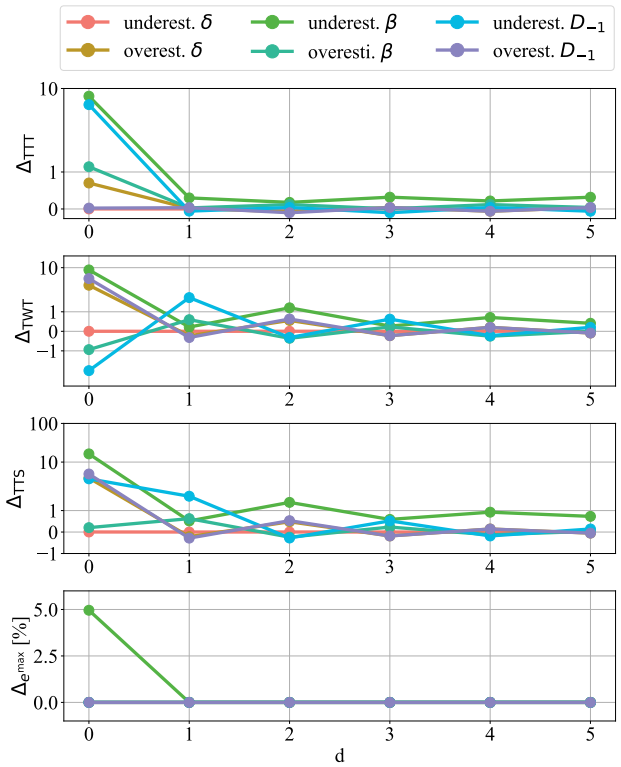

Fig. 5: Relative performance of the ILC scheme over 5 iterations with the scenarios in Table II.

values of Δ_{TTT} suggest that the control effect of reducing congestion can be undermined by imprecise knowledge of the parameters. In some cases (e.g., underestimating β), due to wrong estimates, the controller can result in both positive Δ_{TTT} and Δ_{TWT} simultaneously, leading to greater overall TTS. Moreover, the queue length constraints can be violated as well. Remarkably, by exploiting previous data at subsequent steps, ILC is able to converge rapidly towards GT-MPC (within one or two iterations) in all cases, achieving lower Δ_{TTT} (therefore lower TTT), as indicated by the fast convergence of all curves to a neighborhood of 0 value. Moreover, the queue length constraint can always be satisfied. This shows the effectiveness of our ILC approach.

V. CONCLUSIONS

ILC tailored to the CTM-s model is an effective algorithm to perform highway traffic control and mitigate the presence of parameters' identification errors. Numerical experiments show that by leveraging the repetitive traffic pattern, our ILC approach converges to the optimal MPC controller with ground-truth parameters. Our ILC method recovers from the

incorrect initial estimations in a few iterations and outperforms MPC under the same conditions, remarkably, even when the parameter values differ by 20% from the correct ones.

This study focuses on a single highway with one service station. An interesting extension is to use this approach to control more complex road networks with multiple stations, where coordinated control may yield better performance. Another potential direction is developing a nonlinear ILC to address model mismatch introduced by the linear relaxation of the CTM-s model, which inherently contains nonlinear dynamics. Our current formulation requires an extra cost term TTD, which can potentially diverge the controller from the original goal of reducing TTT. With non-linear formulation, we might skip relaxation and remove TTD, and therefore reduce congestion more effectively.

References

[1] E. Commission, *EU Transport in Figures, Statistical Pocketbook*. Publications Office of the European Union, 2022.

[2] R. Diemer and F. Dittrich, *Transport in the European Union: Current Trends and Issues*. Directorate-General for Mobility and Transport of the European Union, 2019.

[3] A. Ferrara, S. Sacone, S. Siri, *et al.*, *Freeway traffic modelling and control*, vol. 585. Springer, 2018.

[4] M. Papageorgiou, C. Diakaki, V. Dinopoulou, A. Kotsialos, and Y. Wang, "Review of road traffic control strategies," *Proceedings of the IEEE*, vol. 91, no. 12, pp. 2043–2067, 2003.

[5] I. Papamichail, M. Papageorgiou, and Y. Wang, "Motorway traffic surveillance and control," *European Journal of Control*, vol. 13, no. 2-3, pp. 297–319, 2007.

[6] M. Papageorgiou and A. Kotsialos, "Freeway ramp metering: An overview," *IEEE transactions on intelligent transportation systems*, vol. 3, no. 4, pp. 271–281, 2002.

[7] F. Vrbanić, E. Ivanjko, K. Kušić, and D. Čakija, "Variable speed limit and ramp metering for mixed traffic flows: A review and open questions," *Applied Sciences*, vol. 11, no. 6, p. 2574, 2021.

[8] C. Cenedese, M. Cucuzzella, A. Ferrara, and J. Lygeros, "A novel control-oriented cell transmission model including service stations on highways," in *2022 IEEE 61st Conference on Decision and Control (CDC)*, pp. 6278–6283, IEEE, 2022.

[9] C. Cenedese, M. Cucuzzella, A. C. Ramusino, D. Spalenza, J. Lygeros, and A. Ferrara, "Optimal service station design for traffic mitigation via genetic algorithm and neural network," *IFAC-PapersOnLine*, vol. 56, no. 2, pp. 1528–1533, 2023.

[10] A. Kamalifar, C. Cenedese, M. Cucuzzella, and A. Ferrara, "A new control-oriented METANET model to encompass service stations on highways," in *2024 European Control Conference (ECC)*, pp. 1387–1392, 2024.

[11] M. Uchiyama, "Formation of high-speed motion pattern of a mechanical arm by trial," *Transactions of the Society of Instrument and Control Engineers*, vol. 14, no. 6, pp. 706–712, 1978.

[12] S. Arimoto, S. Kawamura, and F. Miyazaki, "Bettering operation of robots by learning," *Journal of Robotic systems*, vol. 1, no. 2, pp. 123–140, 1984.

[13] S. Mishra, U. Topcu, and M. Tomizuka, "Optimization-based constrained iterative learning control," *IEEE Transactions on Control Systems Technology*, vol. 19, no. 6, pp. 1613–1621, 2010.

[14] D. H. Owens and J. Hätönen, "Iterative learning control—an optimization paradigm," *Annual reviews in control*, vol. 29, no. 1, pp. 57–70, 2005.

[15] N. Amann, D. H. Owens, and E. Rogers, "Iterative learning control for discrete-time systems with exponential rate of convergence," *IEE Proceedings-Control Theory and Applications*, vol. 143, no. 2, pp. 217–224, 1996.

[16] A. Schöllig and R. D'Andrea, "Optimization-based iterative learning control for trajectory tracking," in *2009 European Control Conference (ECC)*, pp. 1505–1510, IEEE, 2009.

[17] Q. Yu and Z. Hou, "Data-driven predictive iterative learning control for a class of multiple-input and multiple-output nonlinear systems," *Transactions of the Institute of Measurement and Control*, vol. 38, no. 3, pp. 266–281, 2016.

[18] S.-K. Oh and J. M. Lee, "Stochastic iterative learning control for discrete linear time-invariant system with batch-varying reference trajectories," *Journal of Process Control*, vol. 36, pp. 64–78, 2015.

[19] D. Meng and K. L. Moore, "Robust iterative learning control for nonrepetitive uncertain systems," *IEEE Transactions on Automatic Control*, vol. 62, no. 2, pp. 907–913, 2016.

[20] B. Nemec, M. Simonič, N. Likar, and A. Ude, "Enhancing the performance of adaptive iterative learning control with reinforcement learning," in *2017 IEEE/RSJ international conference on intelligent robots and systems (IROS)*, pp. 2192–2199, IEEE, 2017.

[21] D. Liao-McPherson, E. C. Balta, A. Rupenyan, and J. Lygeros, "On robustness in optimization-based constrained iterative learning control," *IEEE Control Systems Letters*, vol. 6, pp. 2846–2851, 2022.

[22] E. C. Balta, D. M. Tilbury, and K. Barton, "Iterative learning spatial height control for layerwise processes," *Automatica*, vol. 167, p. 111756, 2024.

[23] T. Bellemans, B. De Schutter, and B. De Moor, "Model predictive control for ramp metering of motorway traffic: A case study," *Control Engineering Practice*, vol. 14, no. 7, pp. 757–767, 2006.

[24] G. Gomes and R. Horowitz, "Optimal freeway ramp metering using the asymmetric cell transmission model," *Transportation Research Part C: Emerging Technologies*, vol. 14, no. 4, pp. 244–262, 2006.

[25] Nationaal Dataportaal Wegverkeer, "DEXTER Data Exploration + Exporter." https://dexter.ndw.nu/. Accessed: 2024.